How Natural is the Recent Centennial Warming? An Analysis of 2249 Surface Temperature Records

Horst-Joachim Lüdecke, Rainer Link, and Friedrich-Karl Ewert

EIKE, European Institute for Climate and Energy,
PO.Box 11011, 07722 Jena, GERMANY
info@eike-klima-energie.eu
luedecke@htw-saarland.de
Rainer.Link@gmx.info
ewert.fk@t-online.de

—

Electronic version of an article published in International Journal of Modern Physics C, Vol. 22, No. 10, doi:10.1142/S0129183111016798 (2011), copyright World Scientific Publishing Company, www.worldscinet.com.

Abstract. We evaluate to what extent the temperature rise in the past 100 years was a trend or a natural fluctuation and analyze 2249 worldwide monthly temperature records from GISS (NASA) with the 100-year period covering 1906-2005 and the two 50-year periods from 1906 to 1955 and 1956 to 2005. No global records are applied. The data document a strong urban heat island effect (UHI) and a warming with increasing station elevation. For the period 1906-2005, we evaluate a global warming of 0.58 ^{0}C as the mean for all records. This decreases to 0.41 ^{0}C if restricted to stations with a population of less than 1000 and below 800 meter above sea level. About a quarter of all the records for the 100-year period show a fall in temperatures. Our hypothesis for the analysis is - as generally in the papers concerned with long-term persistence of temperature records - that the observed temperature records are a combination of long-term correlated records with an additional trend, which is caused for instance by anthropogenic CO_2, the UHI or other forcings. We apply the detrended fluctuation analysis (DFA) and evaluate Hurst exponents between 0.6 and 0.65 for the majority of stations, which is in excellent agreement with the literature and use a method only recently published, which is based on DFA, synthetic records and Monte Carlo simulation. As a result, the probabilities that the observed temperature series are natural have values roughly between 40% and 90%, depending on the stations characteristics and the periods considered. 'Natural' means that we do not have within a defined confidence interval a definitely positive anthropogenic contribution and, therefore, only a marginal anthropogenic contribution can not be excluded.

Key words: : Surface temperatures, 2249 records, global warming, natural probabilities, detrended fluctuation analysis.

1 Introduction

It is widely accepted that global surface air temperatures have increased in the past 100 years, with a pronounced rise in the last 50 years. However, the question is not yet answered which forcings cause the actual global temperature change. One assumes natural fluctuations, the Atlantic and Pacific Multidecadal Oscillations, increasing green house gases, urban heat island effects (UHI), natural impacts as volcanic eruptions, condensation nuclei generated by cosmic rays in which their concentration is governed by the sun's magnetic field, anthropogenic aerosols from insufficiently filtered coal power plants and further impacts [2], [5], [11], [22], [29], [39], [73], [79], [81]. The global temperature increase in the 20^{th} century is mainly evaluated from global temperature records that are established with special algorithms [6], [12], [30], [33], [63]. On its own, however, local records show a different picture, since cooling, not warming, is found for a high percentage of temperature stations worldwide. We argue that global records are not a feasible tool to examine global temperatures. First of all, the homogenization and grid box procedures used to establish global records are inevitably arbitrary and, therefore, could cause quite different outcomes when applied to identical sets of local records. Secondly, and of main interest here, establishing global records attenuate the extremes of uncorrelated local records. As a consequence, the standard deviation, which is a decisive attribute in our analysis, becomes unrealistically small in global records.

Temperature records are long-term correlated - other denotations are 'persistent' or 'long-term memory' -, which is a well-known phenomenon since a warm day is more likely to be followed by another warm day than by a cold day, and vice versa. Short-term persistence of weather states on a time scale of about one week is caused by general weather situations. Longer-term persistence over several weeks is mostly related to blocking situations that occur when a high pressure system is established and remains in place for many weeks. Persistence over many months, seasons, years, decades, and even longer periods is usually associated with anomaly patterns in sea surface temperatures, and even with the influence of long-term variations in the sun's activity [8], [9], [56], [58], [68], but there is no universal explanation that can be applied to all causes. In long-term correlated records T_i, i = 1,....,N the autocorrelation function

$$C(s) = \frac{1}{\sigma_N^2 \, (N-s)} \sum_{i=1}^{N-s} (T_i - \langle T \rangle_N)(T_{i+s} - \langle T \rangle_N) \tag{1}$$

fades with increasing s according to the power law

$$C(s) \sim s^{-\gamma} \tag{2}$$

where σ^2 indicates the variance, $\langle T \rangle_N = 1/N \sum_{i=1}^{N} T_i$ is the average of the T_i, and s is the time lag. For $\gamma \approx 1$ the record has no persistence at all (complete randomness), for $\gamma \approx 0$ the record becomes unsteady and could never recur in the long term. In temperature records, typical values for the exponent in Eq. (2) are between $0.4 < \gamma < 0.9$.

However, the most important characteristic of long-term correlated temperature records is that they include fluctuations that appear to be deterministic trends, but are actually quite natural. This phenomenon becomes ever more pronounced in records with increasing persistence, i.e. with decreasing exponent γ (Eq. (2)). Therefore, conventional methods based on moving averages can no longer be used with persistent records to separate deterministic trends from natural fluctuations [7], [15], [36]. This is demonstrated in Figure 1.

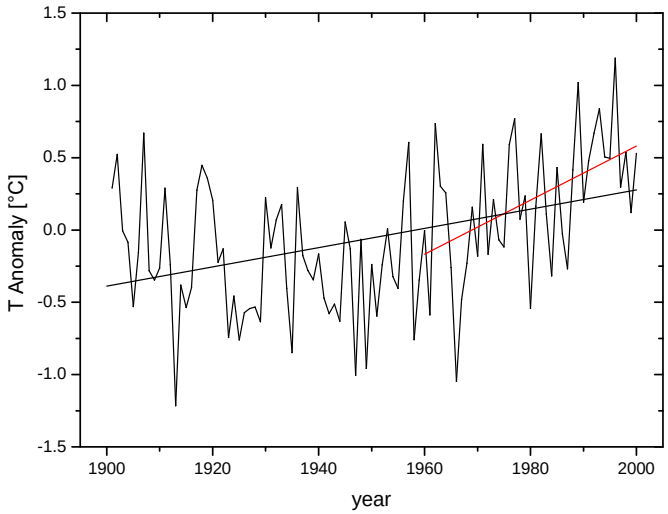

Fig. 1. (color online): A 1200 months (100 years) subsequence with an exponent $\gamma = 0.54$ of the power law in Eq. (2) selected from a synthetic record of $2^{21} = 2{,}097{,}152$ months in length. The record - and all its sub sequences - is purely long-term correlated and do not contain any external trend. Nevertheless, the selected subsequence shows the typical shape of many observed temperature records in the period 1900-2000. We see a modest temperature rise over 100 years (black regression line) with a much stronger ascent during the last 40 years (red regression line).

As a consequence, a conventional examination of a temperature record can not tell us whether an observed change in temperature is natural or an external trend. In particular, the question of how to distinguish a trend caused by anthropogenic greenhouse gases from a natural fluctuation remains unresolved, and has been dubbed the 'detection and attribution problem' [1], [24], [25], [44], [46], [65], [83], [84]. The detrended fluctuation analysis (DFA) as specified in the next paragraph has recently emerged as an effective tool for tackling this problem.

2 Methods: Detrended fluctuation analysis

Long-term correlations in time series are not restricted to temperature records, they are omnipresent in nature. On all time scales, persistence was found in hydrological records, physiological records, economic records, earthquake events and in temperature records [4], [8], [15], [31], [36], [37], [42], [47], [48], [54], [55], [65], [66]. Consequently, the power law of Eq. (2) characterizes the behaviour of persistent records quite generally. However, if the records contain external trends a basic evaluation of the exponent γ in Eq. (2) does not generally yield the correct result. Due to the influence of an external trend in a record the observed persistency becomes wrongly too strong, i.e. the exponent γ becomes too small. Furthermore, the direct calculation of C(s) by Eq. (1) is affected by side effects, for instance, the shortness of the record, and by deterministic trends [45].

Several methods to solve this problem have been developed, the fluctuation method (FA), the detrended fluctuation method (DFA) and wavelet analysis [7], [15], [17], [51], [37], [38], [40], [60], [66], [67], [74], [77], [80]. Among these methods the DFA gives correct results if the record contains external trends. In the following, we confine the description to temperature records and the analysis by DFA. Temperature records are generally available as daily, monthly or annual data. However, the DFA is usually applied to monthly temperatures, not daily ones. Daily data are sensitive to short-term correlations due to general weather conditions of correlation times between days and a couple of weeks, which could influence the fluctuation function of the analyzing methods. On the other side, annual means as temperature data sets are not feasible because the minimum number of data points for DFA is about 600 for numerical reasons. For each calendar month the mean value of the whole record is subtracted from the data and divided by the seasonal standard deviation yielding the normalized record T_i, i=1,...,N applied in our further analysis.

The basic fluctuation analysis FA generates the following profiles as sums over the $\{T_i\}$:

$$Y_j = \sum_{i=1}^{j} T_i \qquad j = 1, ..., N \tag{3}$$

Furthermore, it establishes the standard deviation F(s):

$$F(s) \; = \sqrt{\frac{1}{(N-s)} \sum_{j=1}^{N-s} \left(Y_{j+s} - Y_j\right)^2} \tag{4}$$

For long-term correlated data F(s) of Eq. (4) scales with a power law

$$F(s) \sim s^{\alpha} \tag{5}$$

The exponent α in Eq. (5) is linked to the power law of Eq. (2) by

$$\begin{array}{lll} \alpha = 1 - \gamma/2 & for & 0 < \gamma < 1 \\ \alpha = 0.5 & for & \gamma \geq 1 \end{array} \tag{6}$$

[36]. The hydrology engineer H.E. Hurst was the first to find scaling behaviour in time series and, therefore, α is usually referred to as Hurst exponent [27]. Hurst used a different method - the rescaled range (RS) analysis -, but the α value of Eq. (5) for monofractal data is equivalent to the α of the RS analysis. The exponent α has the limits $0.5 \leq \alpha < 1$, where $\alpha = 0.5$ stands for complete randomness, and $\alpha \approx 1$ for very strong persistence. For $\alpha > 1$, the record becomes unsteady.

The detrended fluctuation analysis of order ν, the DFA_ν, can be assessed as an improved FA which automatically eliminates trends of the polynomial order ν from the profile Y_j and - because Y_j in Eq. (3) integrates the record $\{\mathrm{T}_i\}$ - of polynomial order (ν - 1) from the record itself. In DFA_ν, the profile Y_j of Eq. (3) is divided into $\mathrm{N}_s = \mathrm{int}(\mathrm{N/s})$ non-overlapping intervals of equal length s, and in each interval a polynomial $\mathrm{P}(\nu)$ of order ν is evaluated, which provides the best fit for the profile Y_j. Generally, a short segment at the end of the profile remains. In order not to neglect this segment, one repeats the same procedure from the other end of the record resulting in $2\mathrm{N}_s$ segments. In the next step, the new profile Z_j replaces Y_j of Eq. (3):

$$Z_j = Y_j - P_\nu \tag{7}$$

Finally, the new $\mathrm{F}_\nu(\mathrm{s})$ replaces F(s) of Eq. (4):

$$F_\nu(s) \; = \sqrt{\frac{1}{2N_s} \sum_{k=1}^{2N_s} G_k^2(s)} \tag{8}$$

with

$$G_k^2(s) = \frac{1}{s} \sum_{j=(k-1)s+1}^{ks} (Z_j)^2 \tag{9}$$

For long-term correlated data, the fluctuation function $\mathrm{F}_\nu(\mathrm{s})$ scales like F(s) in Eq. (5) with the same exponent α. It should be stressed that the numerous mechanisms that generate persistence in temperature records induce a consistent scaling behaviour as in Eq. (5) or in Eq. (8). But, in contrast, neither Eq. (2) nor a power law of the fluctuation of the FA or DFA says anything about its origin. We only use DFA_2 here, so for shortness DFA denotes DFA_2 and α denotes $\alpha(\mathrm{DFA}_2)$ in the following. It is useful to depict $\mathrm{F}_\nu(\mathrm{s})$ in Eq. (8) as function of s in a log-log diagram, which enables a basic evaluation of α as the slope of the respective graph. Examples of $\mathrm{F}_2(\mathrm{s})$ graphs are given in Figure 2 for the stations Trelew-Argentina, Hohenpeissenberg-Germany, Abilene-USA, Durban-South-Africa, and Tokyo-Japan.

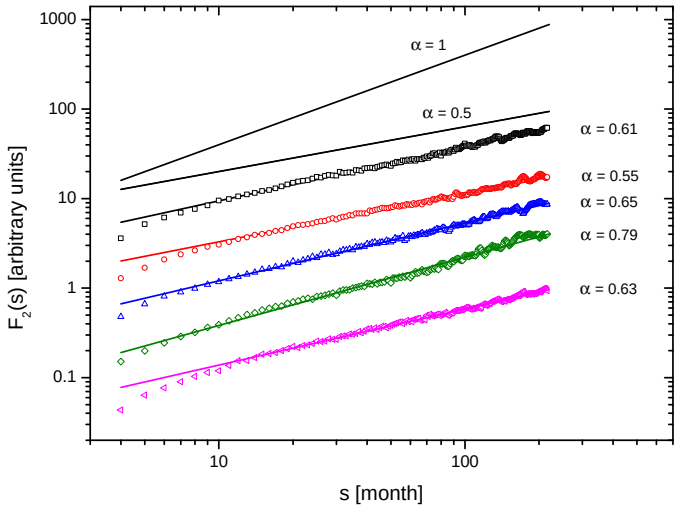

Fig. 2. (color online): $F_2(s)$ of the DFA for the following records from our record pool (top to bottom): Trelew-Argentina, $\alpha = 0.61$; Hohenpeissenberg-Germany, $\alpha = 0.55$; Abilene-USA, $\alpha = 0.65$; Durban-South-Africa, $\alpha = 0.79$; and Tokyo-Japan, $\alpha = 0.63$. The graphs have been shifted for clarity: the lines with $\alpha = 0.5$ and $\alpha = 1$ are for comparison. The downward bend of the few first points in $F_2(s)$ is a known numerical effect.

3 Methods: Probabilities

In the following, we are interested in the probability that in a long-term correlated record with a Hurst exponent α a temperature change Δ appears as a natural fluctuation. Δ is in general the temperature difference of a linear regression line through the record, which is here generally 100 years or 50 years long. Furthermore, we evaluate the standard deviation around the regression line σ and consider the (dimensionless) relative temperature change Δ/σ as the gauge that characterizes the temperature change we are interested in. We thereby follow [44], [46] where it is reported that the common standard deviation can be effected by a trend and, therefore, should not be applied here. Consequently and throughout this paper, we denote Δ as the temperature change of a linear regression line, σ as the standard deviation around the line, and Δ/σ as the authoritative relative temperature change.

If a record contains an external trend, the Hurst exponent of FA is in general higher than that of DFA, but this does not answer the question of how much the record has become unnatural. However, the main matter of interest here is the probability whether an observed 100-year (or a 50-year) temperature change Δ

is a natural fluctuation. 'Natural' denotes that there is no definite anthropogenic trend in the record. For our purpose, the exceedance (cumulative) probability is the adequate tool as the probability W(x) that 'events' $\geq$ x occur. In this study x = Δ/σ represents the relative temperature change in the observed time period. The exceedance probability W(Δ/σ) is not restricted to positive Δ/σ values. If one begins, by definition, with cooling, the exceedance probability of natural records converges to the theoretical limit of W = 1 for extremely strong negative Δ/σ values and decreases with increasing Δ/σ values. In the following, numerical examples of W(Δ/σ) for long-term correlated records with a Hurst exponent of $\alpha = 0.7$ are given as demonstration: W(-5) = 0.99999, W(-1) =0.902, W(-0.4) = 0.697, W(0) = 0.5, W(0.4) = 0.303, W(1) = 0.0983, W(5) = 0.00001. The value W(0) = 0.5 reflects the fact that in natural records we have equal fractions of records with warming and cooling. The following general relation is valid for natural records

$$W\left(-\Delta/\sigma, \alpha\right) = 1 - W\left(\Delta/\sigma, \alpha\right) \tag{10}$$

Eq. (10) verifies again equal fractions with positive and negative Δ/σ values in natural records. If values of W over 0.5 belong to cooling, an exceedance probability of 0.9 would be as significant as of 0.1 for warming.

The latest method to evaluate numerically the exceedance probability W for natural records in a systematic way is a combination of DFA, synthetic records, and Monte Carlo simulations [44], [46]. In principle, this method generates large - generally 2^{21} = 2,097,152 data points in length - long-term correlated synthetic records and evaluates from these long records n short sub sequences for the period under consideration, in our case, 100 or 50 years, each with the same local measured Hurst exponent α as evaluated by DFA for a certain observed record (in general, the α values of sub sequences are similar but not compulsory identical with the α of the long record). For statistical reasons, the number n must be sufficiently large. In the stack of n synthetic records, what is counted is the number z of records with warming equal to or higher than Δ/σ. As a result, the fraction z/n yields the exceedance probability W(Δ/σ, α) for positive Δ/σ values in natural records. By systematically varying Δ/σ and α, the authors of [44] found that their results could be expressed empirically by the following analytic approximation for $\Delta/\sigma > 0$:

$$W\left(\Delta/\sigma, \alpha\right) = C \cdot \exp\left[-B\left(\alpha\right)\left(\Delta/\sigma - 0.2\right)\right] \tag{11}$$

For a period of 50 or 100 years the following parameters are valid: C = 0.8 for 50 years and 1.15 for 100 years; $B\left(\alpha\right) = D\alpha^{-\delta}$ with D = 1, $\delta = 2$ for 50 years, and D = 1.26, $\delta = 2.5$ for 100 years. Eq. (11) holds for W $\leq$ 0.1 and is reported to be a good approximation. For W(Δ/σ, α) > 0.1, a continuation of Eq. (11) was yielded using the error function [44]. For simplicity, if we later refer to Eq. (11) this continuation is included. To validate Eq. (11), we used our own Monte Carlo simulation to compare the approximation with an algorithm based on the standard Fourier-Filtering method for generating synthetic records [75]

and found good accordance with some selected combinations of Δ/σ and α. The approximation of Eq. (11) is completed for negative Δ/σ values by Eq. (10).

In our analysis, we used this approach. Figure 3 depicts the approximation of Eq. (11) for the period of 1200 months. It is demonstrated, for instance, if we were to choose $\Delta/\sigma \approx 1$ and $\alpha \approx 0.7$, then we would read an exceedance probability $\mathrm{W}(\Delta/\sigma,\ \alpha) = \mathrm{W}(1,\ 0.7) \approx 0.1$ and furthermore by applying Eq. (10) of W(-1, 0.7) ≈ 0.9. Hence, the 10% percentage of long-term correlated or detrended real records with $\alpha \approx 0.7$ and 100 years in length shows warming at magnitudes $\geq (\Delta/\sigma \approx 1)$. Further, the 90% percentage of records shows a relative temperature change $\geq (\Delta/\sigma \approx -1)$ and, conversely, the 10% percentage of records a cooling at magnitudes $\leq (\Delta/\sigma \approx -1)$.

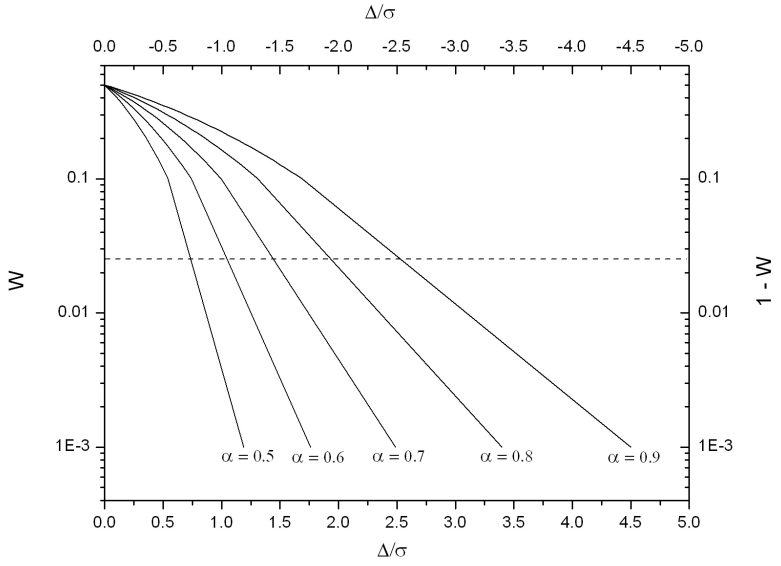

Fig. 3. With the lower x-axis belonging to the left y-axis: Exceedance probabilities $\mathrm{W}(\Delta/\sigma,\ \alpha)$ that relative temperature changes equal to or higher than Δ/σ occur in long-term correlated temperature records - and in detrended real temperature records - of 100 years' duration due to Eq. (11). W can increase by several orders of magnitude when α increases. Therefore, a rise of $\Delta/\sigma > 0$, which is very unlikely for small α values, becomes quite normal for larger ones. The dashed line represents the $(1-2{\cdot}0.025) = 0.95$ confidence interval. Relative trends Δ/σ with $0.025 \leq \mathrm{W} \leq 0.975$ are considered as natural, i.e. as not containing a definitely positive anthropogenic trend. With the upper x-axis belonging to the right y-axis the graph is extended to the cooling domain.

The use of the approximation in Eq. (11) for the analysis of real temperature records that are detrended by DFA is based on the hypothesis that real records

are long-term correlated with an additional trend. Furthermore, for the analysis the trend is assumed to be linear. In order to distinguish between a natural fluctuation and an external trend, a confidence level "a" is needed. Consequently, the domain $0 < W < a$ and $(1 - a) < W < 1$ is considered to include external trends. On the other hand, relative trends in the (1 - 2a) confidence interval a≤W≤(1-a) are regarded as natural. However, 'natural' has to be specified in more detail as follows. If, to cite an example, we were to observe a record detrended by DFA that gives W = 0 the record could be indeed natural. Though, it could also be a mixture of a natural record with W = 1 - a and a strong anthropogenic warming trend or a mixture of a natural record with W = a and a strong negative (cooling) anthropogenic trend. As a consequence, 'natural' applied for a ≤ W ≤ (1-a) means that we do not have within the (1-2a) confidence interval a definitely positive anthropogenic contribution in the record and, therefore, a vanishing anthropogenic contributions must not be excluded. For the sake of a better comprehensibility we prefer to use in the following 'natural' instead of this correct but somewhat clumsy explanation. We defined - to some extent subjectively - the confidence level of a = 0.025, which corresponds to a confidence interval of (1-2a) = 0.95 in accordance with general practice.

However, the basic probability P that n observed records of a group are 'natural' or 'not natural' is of main interest here. For this purpose we evaluate for each distinct record the relative temperature change Δ/σ, the Hurst exponent α by DFA, and the exceedance probability W due to Eqs. (10) - (11). Next, we count the number n_{not_nat} of the records that comply with $W < a$ or $W > (1-a)$ and the number n_{nat} that comply with a ≤ W ≤ (1-a). Hence,

$$P_{not\_nat} = n_{not\_nat}/n \tag{12}$$

yields the probability that the n records of the appropriate group are not natural in the confidence interval (1 - 2a) and, conversely,

$$P_{nat} = n_{nat}/n = (1 - P_{not\_nat}) \tag{13}$$

that they are natural.

4 Application: Data basis, filtering, and basic data characteristics

The Goddard Institute for Space Studies of the National Aeronautics and Space Administration (GISS/NASA) provides about 7500 surface temperature records as unadjusted monthly means and adjusted annual ones, together with the most important characteristics of the stations [19]. The records differ in length and contain more or less voids in the majority of cases. In order to obtain the highest number of available and reliable records, we selected monthly records that comprised at least the 100-year period of 1906-2005, the two 50-year periods of 1906-1955 and 1956-2005, and where voids are below 10.5%. To apply DFA, the

voids must be filled, which was done here by linear interpolation. The GISS applied a somewhat more sophisticated interpolation to evaluate the annual means. However, our annual means based on linear interpolated monthly data hardly differ from the annual GISS means. Our limit of a maximum of 10.5% admissible voids was evaluated by numerical experiments. At first, in records with no voids, we evaluated the Δ/σ values, and the Hurst exponents α by DFA. Next, we removed in the unaffected records data at random positions and also in lumped areas, refilled them using linear interpolation, and evaluated again Δ/σ and α.

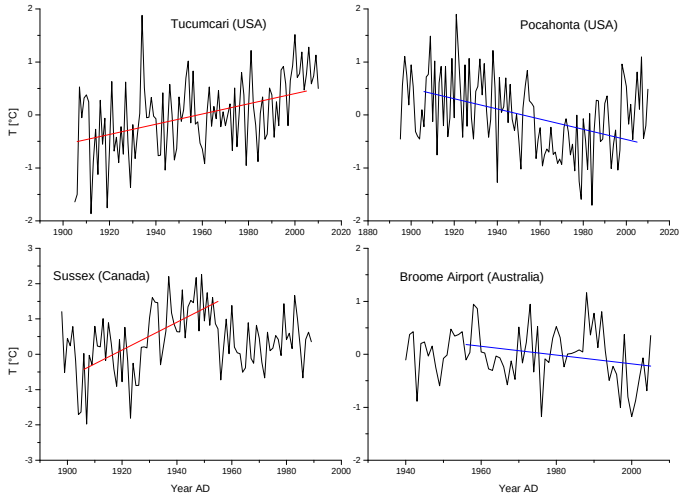

Fig. 4. (color online): Quite different temperature progressions are characteristic for temperature records worldwide. The linear regression lines of the records Tucumcari and Pocahonta are for the period 1906 - 2005, of the record Sussex for 1906 - 1955 and of the record Broome Airport for 1955 - 2005.

We then ascertained that up to 15% of refilled voids still resulted in a correct Hurst exponent α and a correct relative temperature change Δ/σ, with both a maximum error margin of 3%. To be on the safe side we finally restricted our choice further to a maximum of 10.5% admissible voids. The outcome of our selection was 1129 records from 1906-2005 (group A), 427 records from 1906-1955 (group B), and 693 records from 1956-2005 (group C). To both groups B and C, we also added the $2 \cdot 1129 = 2258$ records from group A that were 50 years in length. Figure 4 shows four records as a demonstration of the variety of local temperature series in our data pool.

In the following, we select subgroups of the groups A, B, and C under the station criteria of site, hemisphere, population, and elevation above sea level that are noted in Table 1.

Period	Group	Site	Hemis-phere	Population	Elevation m.a.s.l.	Number of Records
1906-	A1	-	-	400,000	-	1129
2005	A2	Land	-	220,000	-	867
	A3	Ocean	-	1,000,000	-	262
	A4	-	NH	400,000	-	1100
	A5	-	SH	940,000	-	29
	A6	-	-	< 1000	-	581
	A7	-	-	< 1000	≤ 800	461
1906-	B1	-	-	-	-	1556
1955	B2	Land	-	-	-	1124
	B3	Ocean	-	-	-	432
	B4	-	NH	-	-	1431
	B5	-	SH	-	-	125
1956-	C1	-	-	340,000	-	1822
2005	C2	Land	-	216,000	-	1290
	C3	Ocean	-	640,000	-	532
	C4	-	NH	331,000	-	1696
	C5	-	SH	451,000	-	126
	C6	-	-	< 1000	-	890
	C7	-	-	< 1000	≤ 800	686

Table 1: Characteristics of the record groups applied in this study. Land = stations more than 30 km from an ocean; Ocean = stations less than 30 km from an ocean; NH/SH = stations in the northern/southern hemisphere; Population = population mean of the group; m.a.s.l. = meter above sea level.

Figure 5 depicts the frequencies of station population, elevation, latitude, and temperature change Δ in the 100-year period 1906-2005 for the 1129 records of group A1. The latitude frequencies in the left lower panel of Figure 5 show an extreme concentration of temperature stations in the northern hemisphere. Any homogenization or grid box procedures used to evaluate global records are therefore prone to uncertainties caused by the disproportionate density of stations around the globe. Figure 6 depicts the temperature change Δ against station population, Figure 7 the temperature change Δ against station elevation. Notably, the elevation warming is corroborated for three mountain stations [38]. However, apart from UHI and elevation warming, additional warm biases arise in the second 50 years of the 20th century.

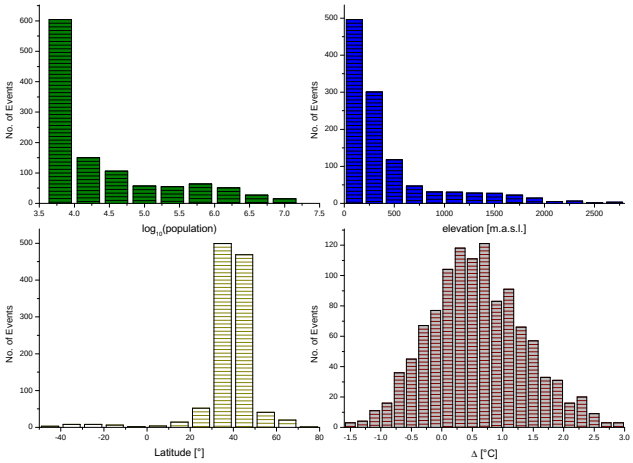

Fig. 5. (color online): Number of events for 1129 temperature records in the 100-year period 1906-2005 of group A1 (Table 1): left upper panel = station population; right upper panel = station elevation above sea level; left lower panel = station latitude; right lower panel = temperature change Δ of linear regression lines.

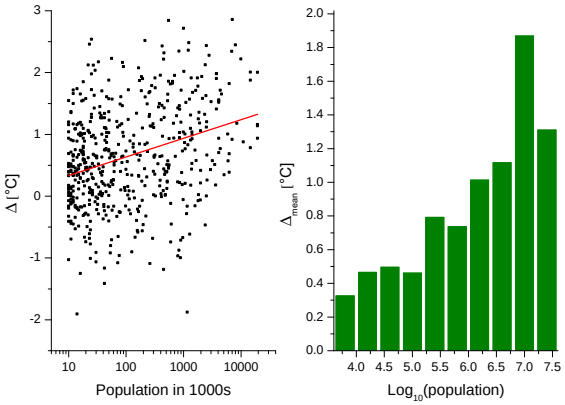

Fig. 6. color online): UHI in 1129 records of the 100-year period 1906-2005 (group A1, Table 1): Left panel: temperature change Δ against station population with linear regression line (red). Right panel: Δ_{mean} values against Log_{10} of station population as a column diagram.

There are mentioned in particular: The screen coating changes in the 1980s, the introduction of the new HO-83 thermometer in the 1990s, new screen elevations above the surface, authoritative changes to the screen neighbourhood (bituminization, air conditioning), as well as changes in land-use, alteration of the algorithms that establish global records, and the reduction in stations from about 6000 formerly to 1500 today, beginning in the mid-1970s [3], [13], [18], [21], [26], [32], [35], [43], [62], [64], [76], [82]. Our finding of an articulate UHI effect is corroborated among others by [10], [57], [72], [76], [79], [81], [82] and is in conflict with the results of [23], [34], [59], [61].

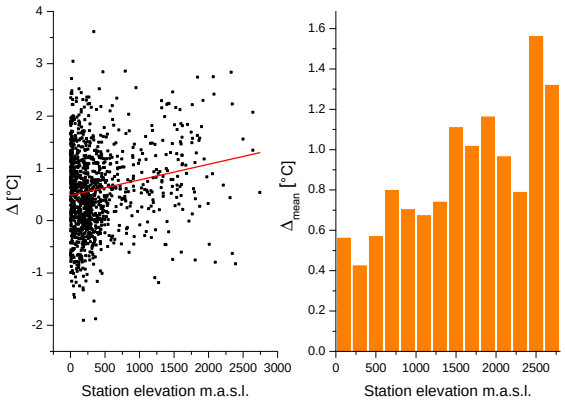

Fig. 7. (color online): Warming due to increasing station elevation in records of the 100-year period 1906-2005 (group A1, Table 1): Left panel: temperature change Δ against station elevation in meter above sea level with linear regression line (red). Right panel: Δ_{mean} values against station elevation as a column diagram.

For comparison, Figure 8 depicts global temperature curves as anomalies. The global record (black) in the left panel of Figure 8 is the mean of the 1129 records of group A1 (Table 1). This record shows that the decade 1995-2005 was the warmest, but that the 1930s were rather similar. Regarding UHI and further warm biases caused by new characteristics of the screens in the second 50 years of the 20^{th} century (see paragraph 5 for relevance), the 1930s could also be assessed as the warmest decade in the 20th century [13]. The linear regression lines reveal two shorter rises for both the interim periods 1901-1934 and 1979-2010, and one longer fall in temperature for the period 1934-1979. The second curve (green) in the left panel of Figure 8 depicts a global record yielded by GISS [20] with an unusual low standard deviation compared with both the local records of our data pool and our global record (black). The probable reason for the low standard deviation was already noted in the introduction (paragraph 1). With regard to the GISS record, the 1930s have distinctly lower temperatures than

the 2000s and the well known maximum of the year 1998 is missing. However, GISS gives no further details about the procedures to establish its global records except for an annotation about the elimination of outliers and homogeneity adjustments. Global records should therefore be considered with care because they could depend on an inevitably arbitrary selection and different algorithms. Consequently and as already stressed earlier, we did not use global records in this study.

From 1998 on, the global temperatures begin again to drop. This also conforms to [71] and the data recorded by HADCRUT 3GL, RSS, GISS, and UAH, which at the least show temperature series as remaining flat. With regard to the period 1998-2010, our selection contains a total of 1386 records that have no voids at all and a population of less than 1000. The mean of the temperature changes for these records shows a clear-cut fall, with Δ_{mean} = -0.34 ^{0}C for the period 1998-2010 and Δ_{mean} = -0.15 ^{0}C for the period 2000-2010.

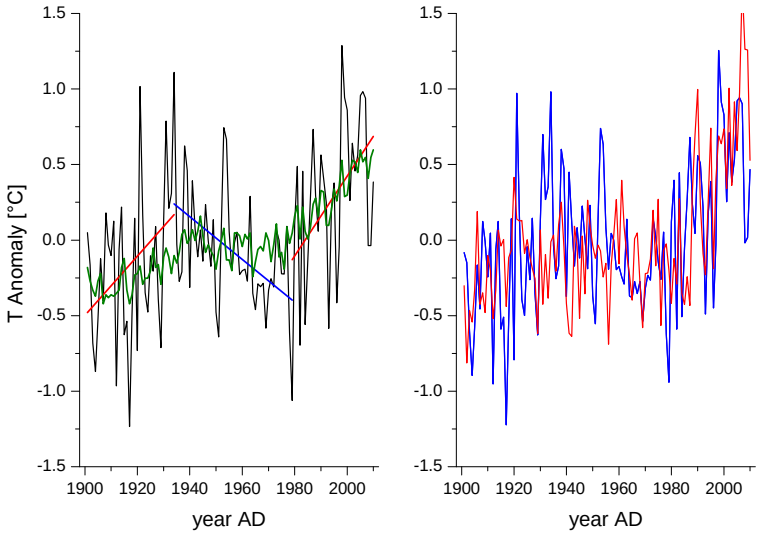

Fig. 8. (color online): Left panel: An own global record evaluated from 581 stations, each in areas with populations of under 1000 (group A6, Table 1), with linear regression lines for the interim periods 1901-1934, 1934-1979, and 1979-2010 (black). The record was evaluated by basic averaging and normalizing local records; global record provided by GISS [20] (green). Right panel: Own global record of stations east of Greenwich, i.e. 961 records of the 1129 records in group A1 (blue); Own global record evaluated from stations west of Greenwich totaled 168 records in group A1 (red). The difference of the GISS global curve and our global record in the left panel and the differences of the two curves in the right panel demonstrate the sensibility of global records on station's selection and on the procedures to establish them.

5 Application: Persistence, and natural probabilities of the observed temperature courses

Figure 9 shows the frequencies of the DFA Hurst exponents α for two subgroups within the 1129 records of group A1 (see Table 1 in paragraph 4), one for locations less than 30 km from an ocean, and the other for locations over 30 km from an ocean.

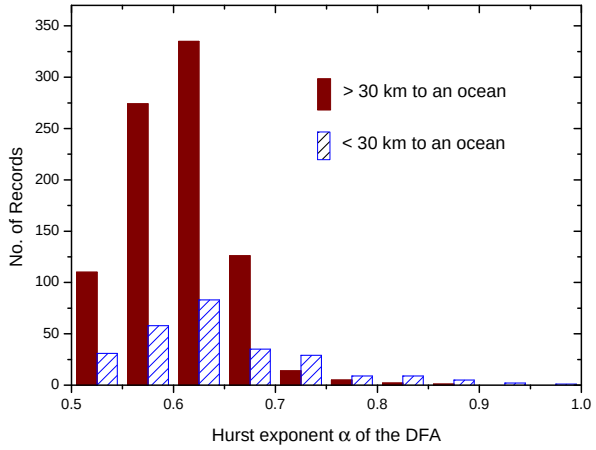

Fig. 9. (color online): Frequencies of the DFA Hurst exponent α for 1129 records of the 100-year group A1 specified in Table 1 of paragraph 4: 867 records of stations over 30 km from an ocean (brown), and 262 records of stations less than 30 km from an ocean (dashed blue).

In the literature a Hurst exponent $\alpha \approx 0.65$ is reported for land stations and evaluated using different methods, including wavelet analysis, FA, and DFA [16], [28], [37], [40], [44], [46], [65]. Island stations generally have a higher Hurst exponent of $\alpha \approx 0.75$. This is explained as being due to the stronger influence of long-term oscillations like AMO or PDO near an ocean [14]. In most papers, monthly records of up to 120 years are employed. The authors of [14] explored 95 instrumental records going back 50 to 120 years from stations all over the globe. They could not find indications of a warming of the atmosphere in the vast majority of cases. Detrended fluctuation analysis (DFA) and exhaustive Monte-Carlo simulations were used to examine 17 local records and 15 global records for both the recent 50-year period and the longer 100-year period, as well as a further 13 local records from different parts of the world covering only the last 50 years [44]. The results showed that the exceedance probabilities of the observed temperature changes widely scattered, ranging from $< 0.01\%$ over 50%

to very near the theoretical limit of 100%. Further, the authors could give only weak support for the conventional thesis that the warming trend in the last 50 years changed its character compared with the first 50 years of the 20^{th} century.

In our study, we evaluated for each distinct record the relative temperature change Δ/σ, the Hurst exponent α by applying DFA, and the exceedance probability W due to Eqs. (10) - (11) which, in the following, is given in percent. The results are shown in the following Table 2 (see also Table 1 in paragraph 4).

Period	Group	Cooling [%]	Δ_{mean} [^{0}C]	$(\Delta/\sigma)_{mean}$	α_{mean}	W_{mean} [%]	P_{nat} [%]
1906-	A1	23	0.58	0.88	0.61	26	58
2005	A2	26	0.51	0.68	0.61	29	64
	A3	13	0.84	1.54	0.64	17	39
	A4	23	0.59	0.89	0.61	26	58
	A5	41	0.26	0.53	0.72	43	55
	A6	25	0.52	0.70	0.61	29	62
	A7	28	0.41	0.53	0.62	32	68
1906-	B1	18	0.49	0.74	0.64	26	83
1955	B2	17	0.50	0.70	0.62	26	84
	B3	21	0.47	0.82	0.68	28	80
	B4	15	0.54	0.80	0.63	24	82
	B5	53	-0.01	-0.02	0.74	52	92
1956-	C1	4	0.9	1.55	0.64	10	54
2005	C2	3	1.0	1.51	0.62	8	52
	C3	7	0.9	1.64	0.69	13	57
	C4	3	1.0	1.57	0.63	9	52
	C5	17	0.6	1.27	0.72	23	72
	C6	4	0.9	1.45	0.63	10	57
	C7	4	0.9	1.41	0.64	10	60

Table 2: Results of the persistence analysis. Cooling = percentage of records that show cooling instead of warming; Δ_{mean} temperature change of a linear regression line; $(\Delta/\sigma)_{mean}$ = relative temperature change; α_{mean} = Hurst exponent of the DFA analysis; W_{mean} = exceedance probability due to Eqs. (10) - (11); P_{nat} = probability that the observed temperature course is natural; $_{mean}$ = mean of the records in the associated group.

Table 2 shows that the cooling fraction of all groups is below 50%, except for group B5 where we have more records with cooling than warming. The W_{mean} of all groups lies well outside the domain for external trends $W < 2.5\%$ or $W > 97.5\%$. This is by itself an indication that global warming from 1906-2005 was to a high degree natural. The differences in the Δ_{mean} values between the group A1 and A6 corroborate the strong UHI already indicated in Figure 6 of paragraph 4. In particular, both the small cooling fraction of 13% and the smallest W_{mean} of 17% for A3 are probably caused by an unusual strong UHI, since

A3 has the highest station population (see Table 1 in paragraph 4). The maximum W_{mean} is observed for group A5 in the southern hemisphere, but applies only to 29 stations (see Table 1 in paragraph 4). Figure 10 depicts the observed exceedance probabilities W in percent for positive Δ/σ values and (100 - W) for negative Δ/σ values of the groups A1, A6 and A7. They are evaluated by basically counting all the records of the appropriate groups with values $\geq \Delta/\sigma$. The theoretical graphs for purely auto correlated records of the fixed values $\alpha = 0.61$ and $\alpha = 0.75$ due to Eqs. (10) - (11) are shown in Figure 10 as further comparison.

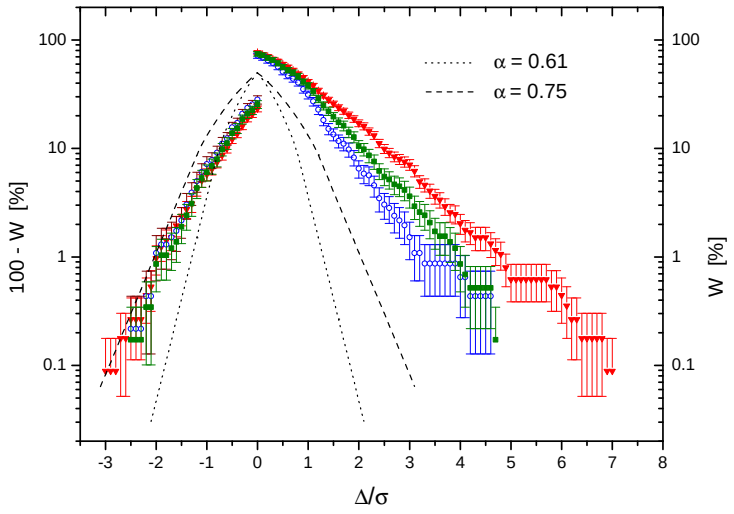

Fig. 10. (color online): Observed exceedance probabilities W in percent for group A1 (all stations, red filled triangles), A6 (stations below 1000 population, green filled squares), and A7 (stations $<$ 1000 population and $<$ 800 meter above sea level, blue open circles) evaluated by counting the appropriate records with values $\geq \Delta/\sigma$. The left y-axis refers to negative Δ/σ values, the right y-axis to positive ones. The dotted and the dashed lines are the theoretical graphs for long-term correlated records with $\alpha = 0.61$ and $\alpha = 0.75$, derived from Eqs. (10) - (11). The graphs for A1 and A6 solely differ in population, and for A1 and A7 both in population and station elevation. Hence, the gap between the graphs of A1 and A6 for $\Delta/\sigma > 0$ is exclusively caused by the UHI. The gap between the graphs of A6 and A7 is caused exclusively by different station elevations.

Figure 10 reveals a similar cooling for the groups A1, A6 and A7, but the warming band shows distinct differences. We see a gap at $\Delta/\sigma = 0$ because there are more records with warming than with cooling. The only difference between A1 and A6 is the UHI and between A6 and A7 the station elevation. A strong UHI has already become manifest in the smaller Δ_{mean} value for A6 compared with A1 (see Table 2) and in Figure 6 of paragraph 4. Now again, Figure 10 depicts the distinct UHI as the gap between the graphs of A1 and A6 for $\Delta/\sigma > 0$. The theoretical curves for long-term correlated records derived from Eqs. (10) - (11) show that $\alpha \approx 0.75$ could be possibly a more realistic value for the Hurst exponent of the Earth as a whole because 2/3 of its surface is covered by water. This assumption is backed up by the higher α values for the groups A3 and A5 (see Table 2). However, the higher the α values, the greater the appropriate W_{mean}. In the warming domain, the gap between the theoretical line for $\alpha = 0.75$ and the A7 graph in Figure 10 could be explained by warming due to anthropogenic greenhouse gases, and additional warm biases caused by authoritative alterations of the station characteristics beginning in the 1970s, and, most notably, the activity of the sun [39], [41], [49], [50], [52], [53], [68], [69], [70], [73], [78]. However, all these impacts can not be separated from each other.

6 Conclusion

In this paper, we have used 2249 unadjusted monthly temperature records of 100 and 50 years in length and evaluated the temperature changes for the periods 1906-2005, 1906-1955, and 1956-2005. Our analysis was based exclusively on local records and applied DFA, Monte Carlo methods and synthetic records. The main results and conclusions are the following.

a) The mean of all stations shows 0.58 ^{0}C global warming from 1906 to 2005. If we consider only those stations with a population of under 1000 and below 800 meter above sea level this figure drops to 0.41 ^{0}C and would probably decrease even further if we were to take into account the warm biases caused by the worldwide reduction in rural stations during the 1990s, by changes to the screens and their environments, and by the appearance of automatic observing systems.
b) From 1906 to 2005, about a quarter of all records show falling temperatures. This in itself is an indication that the observed temperature series are predominantly natural fluctuations. 'Natural' means that we do not have within a defined confidence interval a definitely positive anthropogenic contribution and, therefore, only a marginal anthropogenic contribution can not be excluded. We evaluated - with a confidence interval of 95% - the probability that the observed global warming from 1906 to 2005 was a natural fluctuation as lying between 40% and 70%, depending on the station's characteristics. For the period of 1906 to 1955 the probabilities are arranged between 80% and 90% and for 1956 to 2005 between 60% and 70%.

c) By separating stations into specific station groups, such as those with a defined minimum population, a strong UHI and elevation warming can be identified.
d) The vast majority of temperature stations are found on land and in the northern hemisphere, and have Hurst exponent of $\alpha \approx 0.63$ in such locations. However, two thirds of the Earth are covered with water, and the relatively few stations on islands or near oceans have higher Hurst exponent of $\alpha \approx 0.7$. Therefore, a real exponent for the entire Earth could be somewhat higher than $\alpha \approx 0.63$. Records with higher exponents embody even higher probabilities for natural fluctuations.

7 Acknowledgement

We thank S. Lennartz (University Edinburgh - Scotland) who attended our study from the beginning until closing. Furthermore, we thank A. Bunde (Department of Theoretical Physics III, University of Giessen - Germany) and K.O. Greulich (Fritz Lipmann Institute, University of Jena - Germany) for many helpful discussions on early versions of the manuscript.

References

1. T. Barnett et al., Detecting and attributing external influences on the climate system: A review of recent advances, *J. Clim.* **18**(9), p. 1291 (2005)
2. F. Biondi, A. Gershunov, and D.R. Cayan, North Pacific Decadal Climate Variability since 1661, *AMS*, Volume 14, Issue 1 (January 2001)
3. A. Block, K. Keuler, E. Schaller, Impacts of anthropogenic heat on regional climate patterns, *Geophys. Res. Lett.* **31**, L12211, DOI:10.1029/2005JD006548 (2004)
4. M.I. Bogachev, I.S. Kireenkov, E.M. Nifontof, and A. Bunde, Statistics of return intervals between long heartbeat intervals and their usability for online prediction of disorders, *New Journal of Physics* **11**, 063036 (2009)
5. T.C. Bond, E. Bhardwaj, R. Dong, R. Jogani, S. Jung, C. Roden, D.G. Streets, and N.M. Trautmann, Historical emissions of black and organic carbon aerosol from energy-related combustion, 1850-2000, *Global Biogeochemical Cycles* **21**, GB2018, doi: 10.1029/2006GB002840 (2007)
6. P. Brohan, J.J. Kennedy, I. Harris, S.F.B. Tett, and P.D. Jones: Uncertainty estimates in regional and global observed temperature changes: a new dataset from 1850, *J. Geophysical Research* **111**, D12106, doi:10.1029/2005JD006548 (2006)
7. A. Bunde, J.W. Kantelhardt, Langzeitkorrelationen in der Natur: von Klima, Erbgut und Herzrhythmus, *Phys. Blätter* **57**, Nr. 5 (2001)
8. A. Bunde, J. Kropp, and H.-J. Schellnhuber, The science of disaster: Climate disruptions, market crashes and heart attacks, *Springer*, Berlin (2002)
9. J.G. Charney, and J.G. de Vore, Multiple flow equilibra in the atmosphere and blocking, *J. Atmos. Sci.* **36**, p. 1205 (1979)
10. X.-L. Chen, H.-M. Zhao, P.-X. Li, and Z.-Y. Yin, Remote sensing image-based analysis of the relationship between urban heat island and land use/cover changes, *Remote Sensing of Environment* **104**, p. 133 (2006)

11. J. Crowley, Causes of Climate Change Over the Past 1000 Years, *science* **286**, p. 270 (2000)
12. CRU, http://www.cru.uea.ac.uk/cru/data/temperature/#sciref (2011)
13. J. D'Aleo, J.A. Watts, Surface Temperature Records: Policy driven Deception?, *Science and Public Policy Institute*, 23.Jan. (2010)
14. J.F. Eichner, E. Koscielny-Bunde, A. Bunde, S. Havlin, and H.-J. Schellnhuber, Power-law persistence and trends in the atmosphere: A detailed study of long temperature records, *Phys. Rev. E* **68**(4), doi:10.1103/PhysRevE.68.046133 (2003)
15. J.F. Eichner, J.W. Kantelhardt, A. Bunde, and S. Havlin, Extreme value statistics in records with long-term persistence, *Phys. Rev. E.* **73**, doi: 10.1103/PhysRevE.73.016130 (2006)
16. J. Feder, Fractals, *Plenum Press*, New York (1988)
17. K. Fraedrich and R. Blender, Scaling of Atmosphere and Ocean Temperature Correlations on Observations and Climate Models, *Phys. Rev. Lett.* **90**, 108501 (2003)
18. R. Gall, K. Young, R. Schotland, and R. Schmitz, The Recent Maximum Temperature Anomalies in Tuscon. Are they real or an instrumental problem, *J. Clim.* **5**, p. 657 (1992)
19. http://data.giss.nasa.gov/gistemp/station_data/ (2011)
20. http://data.giss.nasa.gov/gistemp/tabledata/GLB.Ts+dSST.txt (2011)
21. J.D. Goodridge, Comments on "Regional Simulations of Greenhouse Warming Including Natural Variability", *Bull. Amer. Meteor. Soc.* **77**, p. 1588 (1996)
22. J.M. Halley, Using models with long-term persistence to interpret the rapid increase of Earth's temperature, *Physica A* **388**, p. 2492
23. J. Hansen, M. Sato, R. Ruedy, K. Lo, D.W. Lea, and M. Medina-Elizade, Global Surface Temperature Change, *PNAS* **103**, 14288 (2006)
24. K. Hasselmann, Optimal Fingerprints for the Detection of Time-Dependent Climate Change, *J. Clim.* **6**(10), p. 1957 (1993)
25. G.C. Hegerl, H. von Storch, K. Hasselmann, B.D. Santer, U. Cubasch, and P.D. Jones, Detecting greenhouse-gas-induced climate change with an optimal fingerprint method, *J. Clim.* **9**(10), p. 2281 (1996)
26. K.M. Hinkel, F.E. Nelson, S.E. Klene, and J.H. Bell, The Urban Heat Island in Winter at Barrow, Alaska, *Int. J. Climat.* **23**, p. 1889, DOI: 10.1002/JOC.971 (2003)
27. H.E. Hurst, Long-term storage capacity of reservoirs, *Transactions of the American Society of Civil Engineers* **116** (2447) p. 770 (1951)
28. H.E. Hurst, R.P. Black, and Y.M. Simaika, Long-term Storage: An Experimental Study, *Constable*, London (1965)
29. IPCC, the scientific basis, AR4WG1_CH02, www.ipcc.ch (2007)
30. IPCC, the scientific basis, AR4WG1_CH03, www.ipcc.ch (2007)
31. P.CH. Ivanov, A. Bunde, L.A.N. Amaral, S. Havlin, J. Fritsch-Yelle, R.M. Baevsky, H.E. Stanley, and A.L. Goldberger, Sleep-wake differences in scaling behaviour of the human heartbeat: Analysis of terrestrial and long-term space flight data, *Europhysics Letters* **48**(5), p. 594 (1999)
32. C.G. Jones, and K.C. Young, An Investigation of Temperature Discontinuities introduced by the Installation of the HO-83 Thermometer, *J. Clim.* **8**(2), p. 1394 (1995)
33. P.D. Jones, and A. Moberg, Hemispheric and Large-Scale Surface Air Temperature Variations: An Extensive Revision and an Update to 2001, *J. Clim.* **16**, p. 206 (2003)

34. P.D. Jones, D.H. Lister, and Q. Li, Urbanisation effects in large-scale temperature records, with an emphasis on China, *J. Geophysical Research* **113**, D16122, doi : 10.1029/2008JD009916 (2008)
35. E. Kalnay, and M. Cai, Impacts of urbanisation and land-use change on climate, *Nature* **423**, p. 528 (2003)
36. J.W. Kantelhardt, E. Koscielny-Bunde, H.H.A. Rego, S. Havlin, and A. Bunde, Detecting long-range correlations with detrended fluctuation analysis, *Physica A* **295**, p. 441 (2001)
37. J.W. Kantelhardt, Fluktuationen in komplexen Systemen (Fluctuations in complex Systems), professorial dissertation, University Giessen (Germany), 19. June 2004
38. A. Kiraly, I. Bartos, and I.M. J'Anosi, Correlation properties of daily temperature anomalies over land, *Tellus, Ser. A* **58**(5), p. 593 (2006)
39. J. Kirkby, Cosmic Rays and Climate, *European Organisation for Nuclear Research*, CERN-PH-EP/2008-005 (2008)
40. E. Koscielny-Bunde, A. Bunde, S. Havlin, H.E. Roman, Y. Goldreich, and H.-J. Schellnhuber, Indication of a universal persistence law governing atmospheric variability, *Phys. Rev. Lett.* **81**(3), p. 729 (1998)
41. N.A. Krivova, and S.K. Solanki, Solar variability as an input to the Earth's environment, International Solar Cycle Studies (ISCS) Symposium, 23 - 28 June 2003, Tatranska Lomnica, Slovak Republic. Ed.: A. Wilson. ESA SP-535, *Noordwijk: ESA Publications Division*, ISBN 92-9092-845-X, 2003, p. 275 (2003)
42. J. Kropp, and H.-J. Schellnhuber, In Extremis: Trends, Correlations, and Extremes in Hydrology and Climate, *Springer*, Berlin (2010)
43. H. E. Landsberg, The Urban Climate, International Geophysics Series 28, *Academic Press*, New York (1981)
44. S. Lennartz, and A. Bunde, Trend Evaluation in Records with Long-Term Memory: Application to Global Warming, *Geophys. Rev. Lett.* **36**, L16706, doi:10.1029/2009GL039516 (2009)
45. S. Lennartz, and A. Bunde, Eliminating finite-size effects and detecting the amount of white noise in short records with long-term memory, *Phys. Rev. Lett. E* **79**, p. 066101 (2009)
46. S. Lennartz, and A. Bunde, Distribution of natural trends in long-term correlated records: A scaling approach, *Phys. Rev. E* **84**, 021129 (2011)
47. V.N. Livina, Y. Ashkenazy, Z. Kizner, V. Strygin, A. Bunde, and S. Havlin, A stochastic model of river discharge fluctuations, *Physica A* **330**, p. 283 (2003)
48. V.N. Livina, S. Havlin, and A. Bunde, Memory in the Occurrence of Earthquakes, *Phys. Rev. Lett.* **95**, 208501 (2005)
49. M. Lockwood, R.G. Harrison, T. Woollings, and S.K. Solanki, Are cold winters in Europe associated with low solar activity?, *Environ. Res. Lett.* **5**, 024001, doi:10.1088/1748-9326/5/2/024001 (2010)
50. M. Lockwood, Solar influence on the Earth's climate, ISSI Workshop "Observing & Modelling Earth's Energy Flow", 11. Jan. 2011
51. C. Loehle, Climate change: detection and attribution of trends from long-term geological data, *Ecolog. Model.* **171**, 433-450, doi:10.1016/j.ecolmodel.2003.08.013 (2004)
52. Q.-B. Lu, Cosmic-ray-driven-electron-induced reactions of halogenated molecules adsorbed on ice surfaces: implications for atmospheric ozone depletion, *Physics Reports - Elsevier* **487**, p. 141 (2010)

53. H.-J. Lüdecke, Long-term instrumental and reconstructed temperature records contradict anthropogenic global warming, *Energy & Environment* **22**(6), p. 723 (2011)
54. F. Lux, and M. Ausloos, Market fluctuations I: Scaling, multiscaling, and their possible origins, in "The science of disaster", *Springer*, Berlin, p. 373, chapter 13 (2002)
55. R.N. Mantegna, and H.E. Stanley, An Introduction to Econophysics: Correlations and Complexity in Finance, *Cambridge University Press*, Cambridge (2000)
56. R.A. Monetti, S. Havlin, and A. Bunde, Long term persistence in the sea surface temperature fluctuations, *Physica A* **320**, p. 581 (2003)
57. C.J.G. Morris, I. Simmonds, and N. Plummer, Quantification of the Influences of Wind and Cloud on the Nocturnal Urban Heat Island of a large City, *J. Appl. Meteor.* **40**, p. 169 (2001)
58. T.N. Palmer, Predicting uncertainty in forecasts of weather and climate, *Rep. Prog. Phys.* **63**, p. 71 (2000)
59. D.E. Parker, Large-Scale Warming is not Urban, *Nature* **432**, 290, doi:10.1038/432290a (2004)
60. J.D. Pelletier, and D. L. Turcotte, Self-affine time series: II. Applications and models, *Adv. Geophys.* **40**, p. 91 (1999)
61. T.C. Peterson, Assessment of urban versus rural in situ surface temperatures in the contiguous United States: No difference found, *J. Clim.* **16**, p. 2941 (2003)
62. R. Sr. Pielke, J. Nielson-Gammon, C. Davey, J. Angel, O. Bliss, N. Doesken, M. Cai, S. Fall, D. Niyogi, K. Gallo, R. Hale, K.G. Hubbard, X. Lin, H. Li, and S. Raman, Documentation of Uncertainties and Biases Associated with Surface Temperature Measurement Sites for Climate Change Assessment, *Bull. Amer. Meteor. Soc.* **88**:6, p. 913 (2007)
63. N.A. Rayner, D.E. Parker, E.B. Horton, C.K. Folland, L.V. Alexander, D.P. Rowell, E.C. Kent, and A. Kaplan, Globally complete analyses of sea surface temperature, sea ice and night marine air temperature, 1871-2000, *J. Geophysical Research* **108**, p. 4407, doi:10.1029/2002JD002670 (2003)
64. G. Ren, Y. Zhou, Z. Chu, J. Zhou, A. Zhang, J. Guo, and X. Liu, Urbanisation Effects on Observed Surface Air Temperature Trends in North China, *J. Clim.* **21**, p. 1333, DOI: 10.1175/2007JCLI1348.1 (2008)
65. D. Rybski, A. Bunde, S. Havlin and H. von Storch, Long-term persistence in climate and the detection problem, *Geophys. Res. Lett.* **33**, L06718, doi:10.1029/2005GL025591 (2006)
66. D. Rybski, A. Bunde, and H. von Storch, Long-term memory in 1000-year simulated temperature records, *J. Geophys. Res.* **113**, D02106, doi:10.1029/2007JD008568 (2008)
67. D. Rybski, and A. Bunde, On the detection of trends in long-term correlated records, *Physica A* **388**, p. 1687 (2009)
68. N. Scafetta, P. Grigolini, T. Imholt, J. Roberts, and B. West, Solar turbulence in Earth's global and regional temperature anomalies, *Phys. Rev. E* **69**, 026303 (2004)
69. N.J. Shaviv, J. Veizer, Celestial driver of Phanerozoic climate?, *GSA Today* **3**(7) (2003)
70. S.K. Solanki, I.G. Usoskin, B. Kromer, M. Schüssler and J. Beer, An unusually active Sun during recent decades compared to the previous 11,000 years, *Nature* **431**, 7012, p. 1084 (2004)
71. D.R.B. Stockwell, Recent Climate Observations: Disagreement with Projections, *Energy & Environment* **20**(4), p. 595 (2009)

72. D.R. Streutker, Satellite-measured growth of the urban heat island of Houston, Texas, *Remote Sensing of Environment* **85**, p. 282, doi: 10.1016/S0034-4257(03)00007-5 (2003)
73. H. Svensmark, T. Bondo, and J. Svensmark, Cosmic ray decreases affect atmospheric aerosols and clouds, *Geophys. Res. Lett.* **36**, L15101, doi:10.1029/2009GL038429 (2009)
74. P. Talkner, and R.O. Weber, Power spectrum and detrended Fluctuation analysis: Application to daily temperatures, *Phys. Rev. E* **62**, 150 (2000)
75. D.L. Turcotte, Fractals and Chaos in Geology and Geophysics, 2nd ed., *Cambridge University Press*, Cambridge (1997)
76. A. Velazquez-Lozada, J. E. Gonzales, and A. Winter, Urban heat island effect analysis for San Juan, Puerto Rico, *Atmospheric Environment* **40**, 9, p. 1731, DOI: 10.1016/j.atmosenv.2005.09.074 (2005)
77. R.O. Weber, and P. Talkner, Spectra and correlations of climate data from days to decades, *J. Geophys. Res.* **106** (D17), 20, 131-20, 144 (2001)
78. W. Weber, Strong Signature of the Active Sun in 100 Years of Terrestrial Insolation Data, *Annalen der Physik* **522**, No. 6, p. 372, DOI 10.1002/andp201000019 (2010)
79. Q. Weng, Fractal Analysis of Satellite-Detected Urban Heat Island Effect, *Photogrammetric Engineering & Remote Sensing* **69**, No. 5, p. 555 (2003)
80. K. Yamasaki, L. Muchnik, S. Havlin, A. Bunde, and H.E. Stanley, Scaling and memory in volatility return intervals in financial markets, *PNAS* **102**, no. 26, p. 9424 (2005)
81. X. Yang, Y. Hou, and B. Chen, Observed surface warming induced by urbanization in east China, *J. Geophys. Res.* **116**, D14113, doi: 10.1029/2010JD015452 (2011)
82. L. Zhou, R. Dickinson, Y. Tian, J. Fang, L. Qingziang, R. Kaufman, C. Tucker, and R. Myneni, Rapid Urbanisation warming China's climate faster than other areas, *PNAS* **01**, no. 26, p. 9540 (2004)
83. E. Zorita, T.F. Stocker and H. von Storch, How unusual is the recent series of warm years?, *Geophys.Res.Lett.* **35**, L24706, doi:10.1029/2008GL036228 (2008)
84. F.J. Zwiers, The detection of climate change, in "Anthropogenic Climate Change", p. 163, *Springer*, New York (1999)